Kinetics of Self-Assembled Monolayer Growth Explored via Submonolayer Coverage of Incomplete Films

J. T. Woodward, I. Doudevski, H. D. Sikes, and D. K. Schwartz*

Department of Chemistry, Tulane University, New Orleans, Louisiana 70118

Received: April 17, 1997; In Final Form: July 21, 1997[⊗]

We have studied the growth kinetics of self-assembled monolayers of octadecylphosphonic acid on mica by examining films removed from solution before completion. Atomic force microscope (AFM) images of the quenched films showed islands approximately 2 nm high indicating a growth mechanism consisting of nucleation, growth, coalescence, etc. of dense submonolayer islands. This was consistent with previous in situ AFM studies. Infrared spectroscopy data were consistent with well-ordered alkyl chains and indicated only one type of chain conformation, implying that the areas between islands were bare, not covered with loosely packed disordered molecules. The surface coverage of the submonolayer islands was extracted from AFM images as a function of immersion time for solution concentrations ranging from 0.02 to 2 mM. These data were compared to two common models for adsorption kinetics—diffusion-limited kinetics and adsorption-limited (Langmuir) kinetics. The previously reported quasi-Langmuir−Blodgett deposition process occurring during removal was also taken into account in this modeling. The data were completely inconsistent with the adsorption-limited kinetics and were in reasonable agreement with the functional form for diffusion-limited kinetics. However, the diffusion parameters extracted from the latter fits were much smaller than expected for molecular diffusion in solution and did not scale correctly with solution concentration. We conclude that the island growth is limited by a process that obeys diffusion-like kinetics but not by actual solution diffusion.

Introduction

Recent years have seen an explosion of information of interest in self-assembled monolayers (SAMs) as promising systems for a variety of applications. Although several groups have made important inroads into understanding "equilibrium" SAM structure and phase behavior,[1−6] the original growth process of SAMs is still incompletely understood. In previous work, we have reported a useful model system for growth studies, the SAM deposition of octadecyl phosphonic acid (OPA) on mica substrates.[7,8] Atomic force microscope (AFM) studies, both in situ during growth conditions as well as on quenched incomplete monolayers, suggested that the growth process in this system starts with the nucleation of densely packed submonolayer molecular islands at random locations on the substrate and continues by growth and coalescence of these islands. Experiments on alkyltrichlorosilane SAMs also suggest such an "islanding" mechanism.[6,9] In this paper, we expand upon these previous results, supporting the proposed growth mechanism with detailed contact angle and infrared (IR) spectroscopy data. Moreover, we attempt to quantify the growth kinetics using fractional surface coverage data derived from AFM images of quenched incomplete samples.

There are two main advantages to using incomplete films, as opposed to in situ measurements, for this type of study. First, since there is no need to match the growth kinetics with the appropriate time scale for AFM measurements, we are able to use a large range of solution concentration (spanning 2 orders of magnitude). For in situ studies, the growth kinetics must be slow compared to the image capture rate but must evolve quickly enough that the experiment can be completed before some experimental difficulty arises (e.g., AFM tip becoming blunt or fouled, leakage of liquid cell, bubble passing over sample, experimenter needing sleep). Second, the quality of images obtained under ambient conditions is generally better than that obtained at the solid/liquid interface, allowing a more accurate analysis of surface coverage. Also, since time is not an issue, many areas on the sample can be probed to determine an average value of coverage as well as the degree of uniformity. On the other hand, ex situ observation has two main disadvantages: we cannot follow specific regions of the surface as they evolve and there is a concern that the structure of the quenched film may not represent that of the actual monolayer growing in solution. Qualitatively, this second concern appears to be unfounded in this case, since our in situ studies also showed growth via island formation.[7] Quantitatively, however, there are distinct differences between quenched and in situ surface morphology. We have attempted to explore and quantify these differences—the effect of removal from solution on the incomplete monolayer structure.

Experimental Details

The synthesis of OPA was described previously.[8] Tetrahydrofuran (99.9%, Fisher Scientific; Pittsburgh, PA) was used as a solvent. SAMs were made from solutions with concentrations in the range 2×10^{-5} to 2×10^{-3} M. Water from a Millipore Milli-Q UV+ (Bedford, MA) and hexadecane (99%, Aldrich) were used for contact angle measurements. A holder was fashioned that allowed us to make six samples simultaneously. The substrates were placed in this holder, submerged in OPA solution and removed after immersion for specific times. Upon removal the samples were rinsed in pure THF for 30 s and blown dry with a dry nitrogen stream.

The samples were imaged with a Nanoscope III atomic force microscope (Digital Instruments; Santa Barbara, CA). All images were taken in contact mode using silicon nitride tips. Surface coverage was calculated using the height histogram of

* To whom correspondence should be addressed. Fax: 504-865-5596. Phone: 504-865-5573. E-mail: dks@mailhost.tcs.tulane.edu.

[⊗] Abstract published in *Advance ACS Abstracts,* September 1, 1997.

S1089-5647(97)01338-2 CCC: $14.00

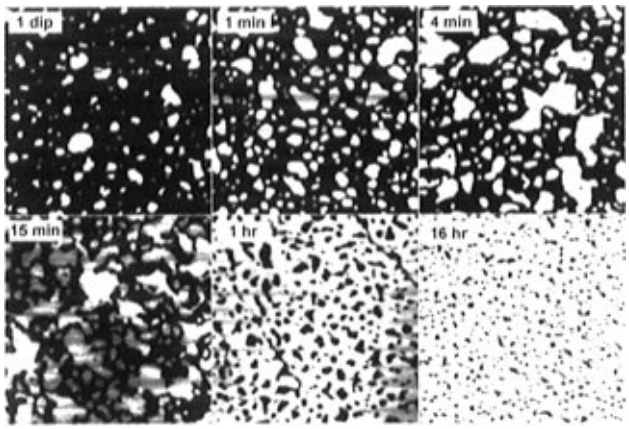

Figure 1. AFM images (1 μm × 1 μm) of incomplete SAMs removed from solution after immersion for various times in a 0.2 mM solution of OPA in THF.

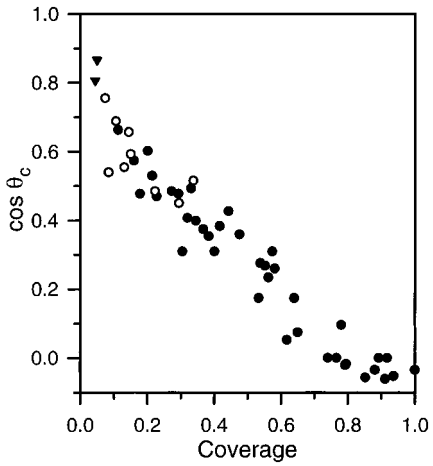

Figure 2. Cosine of the static contact angle of water on various incomplete SAMs is plotted versus the surface coverage measured directly using AFM. Filled triangles refer to films that emerged wet from solution and remained wet until rinsed. Open circles refer to films where the liquid layer wetting the surface after removal from solution immediately broke. Filled circles refer to films that emerged dry from solution.

a given image as described previously.[8] Contact angle measurements were made using a custom-built contact angle goniometer. These measurements were improved over those in our previous publication[8] in that they were performed under saturated vapor pressure conditions. For measurements of the so-called "static" contact angle, we followed a procedure described by Bain et al.[10] in which a 1 μL drop was formed at the end of a needle and brought into contact with the surface. The needle was removed and the contact angle measured. Results were reproducible to within $\pm 2°$.

Infrared absorption data were obtained using a Mattson Cygnus 100 spectrometer in transmission mode with a 6.4 mm pinhole defining the incident beam. Because of the low signal from the submonolayer samples, data were averaged over 3200 scans (about 1.5 h of data collection) for both the film and the bare substrate in order to minimize statistical noise. To obtain background spectra that could be subtracted reliably, we found it necessary to use the same substrate held in the same position in the spectrometer. Accordingly, we fashioned a sample holder that could be reproducibly positioned in the spectrometer to within ± 0.1 mm (much less than the beam size). We first measured the spectrum of the monolayer sample. We then removed the entire holder and placed it in a UV−oxygen cleaner (Boekel Industries) to destroy the monolayer (both sides of the sample were cleaned). The holder was then repositioned within the spectrometer and the background spectrum was measured. Because of the transmission geometry, periodic oscillations due to interference effects were typically observed in the spectra. Depending on the substrate thickness, these oscillations were more or less severe, and with the appropriate choice of substrate the actual peaks could be easily distinguished.

Results and Discussion

A typical sequence of AFM images (from incomplete films) as a function of increasing immersion time is shown in Figure 1. The higher areas ("islands") are approximately 2 nm above the surrounding low areas, generally consistent with the molecular length. No such structures are observed in control experiments in which substrates are immersed in pure solvent. These images are consistent with a picture of monolayer growth in which small islands of densely packed molecules nucleate on the surface and grow by the adsorption of additional molecules. In this model, these islands eventually coalesce, percolate, and finally cover the entire surface. The unchanging height of the islands suggests that the molecules present in even small islands have essentially the same conformation as in the final film. As we discuss below, the quantitative details of the surface morphology as a function of time and solution concentration support this general picture. We also report complementary contact angle and IR data that tend to confirm this model for growth.

Wettability. During removal from deposition solution, a given sample had one of three possible appearances. Samples immersed in low concentration solution for short times emerged wet and remained wetted by solution until rinsed. At the other extreme, samples immersed for fairly long times emerged dry, displaying the autophobicity typical for SAMs. Careful observation uncovered a middle regime where the sample emerged wet originally, but the thin liquid film broke almost immediately, forming a dry area in the central part of the sample that spread rapidly toward the edges. We, therefore, classified samples according to their appearance during removal as "wet", "dry", or "broke". In general, there was reasonable correlation between this appearance and the surface coverage determined from AFM images (see Figure 2). Films that remained wet during removal corresponded to a fractional coverage less than 0.06. Films that "broke" after removal had surface coverage in the range 0.06 to about 0.2. Films that emerged dry from solution generally had coverage greater than 0.2. There was some overlap, however, between the coverage range of films that "broke" and films that emerged dry because of a dependence on solution concentration—in general, films emerged dry from higher concentration solutions at lower coverages.

For very low coverage, the partial monolayer may still be wet by solution at equilibrium. This is the case with the "wet" films. However, at some critical coverage, the spreading coefficient becomes negative and the film should not be wet by solution at equilibrium. Two possible dewetting mechanisms are possible, in general. In one case, the wetting layer can recede from an edge of the sample. This is the case for the samples that emerge "dry." Another dewetting mechanism involves spontaneous nucleation of holes through the wetting layer in the interior of the sample that spread rapidly toward the edges.[11−13] One or many such holes may form. We believe that this is the case for samples that emerge with a thin wetting film that subsequently breaks.

There was also excellent correlation between surface coverage extracted from AFM images and the measured contact angle of water, θ_c, on the film. Figure 2 shows $\cos \theta_c$ plotted versus

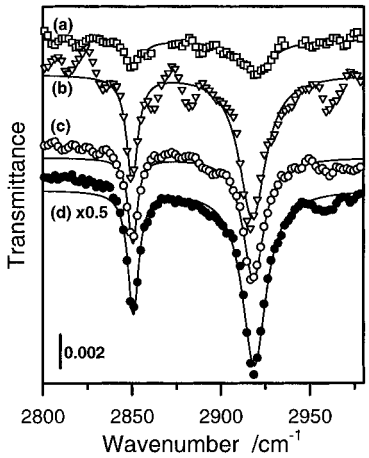

Figure 3. Transmission FTIR spectra of the CH stretching region of several incomplete SAMs compared to that of a cadmium arachidate Langmuir−Blodgett multilayer: (a) SAM with a surface coverage of 0.1; (b) SAM with a surface coverage of 0.3; (c) SAM with a surface coverage of 0.9; (d) cadmium arachidate LB multilayer (absorbance amplitude reduced by one-half).

the measured surface coverage, χ; the dependence is monotonic, nearly linear as expected from the mean-field Cassie equation.[14]

Infrared Spectroscopy. IR data also provide confirmation for the picture of growth implied by AFM images. Figure 3 shows the CH stretch region of the spectrum for three incomplete monolayers. Two peaks are visible, corresponding to the symmetric methylene stretch, $\nu_s(CH_2)$, at about 2850 cm^{-1} and the antisymmetric methylene stretch, $\nu_a(CH_2)$, at about 2920 cm^{-1}. The positions of these peaks are typical for all trans well-ordered alkyl chains[15] and identical with those measured by us on a nine-layer Langmuir−Blodgett film of cadmium arachidate in which the chains are known to be crystalline. This implies that the chains are densely packed and relatively well-ordered inside the islands even at fairly low surface coverage. Also, there is no apparent shoulder in these peaks on the high wavenumber side as might be expected if additional, poorly ordered molecules were present in the areas between islands. This is consistent with the fact that we were routinely able to obtain atomic resolution AFM images of the mica lattice in these "bare" areas. Such images are difficult to attain if a surface is covered by organic "contaminants". The increase in peak intensity with coverage is qualitatively consistent with AFM images.

Quasi-Langmuir−Blodgett Deposition. As we reported previously, the surface coverage of these incomplete films does not extrapolate precisely to zero at zero immersion time.[7] We showed that this phenomenon was due to additional island coverage caused by the process of removing the film from solution. We determined that the deposition occurred during removal and not during insertion by noting the equivalence of the growth kinetics between quenched films grown normally (passing through the solution/air interface during insertion and removal) and those where the clean substrate was initially inserted into pure solvent before OPA molecules were added (passing through the solution/air interface only during removal). A likely source of this additional coverage is quasi-Langmuir−Blodgett (LB) deposition of a molecular layer (a Gibbs monolayer) at the solution/air interface. To verify the existence of such a layer, we measured the surface tension of OPA solution (in THF) as a function of concentration. Figure 4 clearly shows an approximately linear decrease of surface tension with concentration as expected in the limit of low surface density of surfactant.[16] We note that a decrease in surface tension does not, by itself, prove the existence of an adsorbed

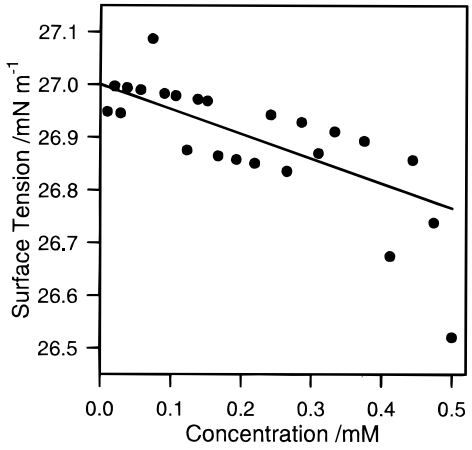

Figure 4. Measured surface tension of OPA dissolved in THF as a function of concentration. The systematic decrease in surface tension is consistent with the presence of an adsorbed Gibbs monolayer at the solution/air interface. The line represents the best linear fit to the data. The error bars are due to the finite precision of the measurement and also incorporate overall uncertainty in the correction due to Wilhelmy plate buoyancy.

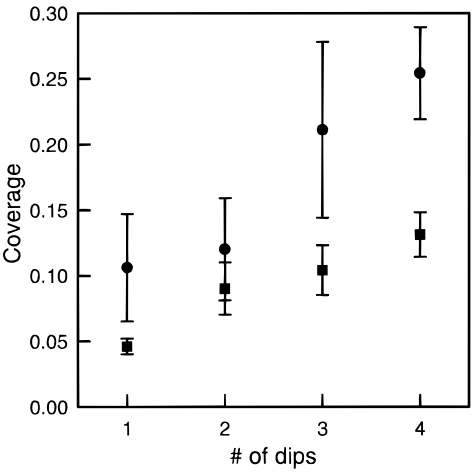

Figure 5. Fraction of the surface covered by islands on "dipped" films determined by image analysis, as discussed in the text, as a function of number of dips: (circles) 0.18 mM solution; (squares) 0.10 mM solution.

monolayer, since a "surface excess" could have a similar effect. In addition, we cannot rule out the possibility that some or all of the coverage added during removal could be due to condensation (clustering) of molecules that were loosely adsorbed to the substrate (between islands) before removal.

We investigated this quasi-LB process by examining films dipped quickly in and out of solution one or more times. Figure 5 shows the measured surface coverage of films dipped one, two, three, or four times into 0.1 or 0.18 mM solution. The coverage increases monotonically with the number of dips and is greater for the larger concentration (presumably because the density of molecules adsorbed at the solution/air interface is greater). The remarkable extent of the coverage of "dipped" films can be appreciated by noting that the coverage of a film dipped 4 times in 0.18 mM solution (total immersion time approximately 4 s) is equivalent to that of a film submerged continuously in the same solution for about 100 s. The islands formed during removal have a distinctive size. Figure 6 compares the island size distribution of a film dipped quickly with films immersed for 120 and 300 s in 0.10 mM solution. The distribution of the dipped film has a prominent peak at about 200 nm^2. This same peak is visible, although less dramatic, in the distributions for the films immersed for longer

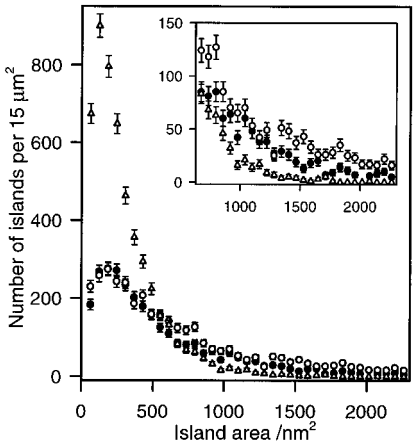

Figure 6. Island area distributions measured on three 1 μm and three 2 μm images of quenched films for 1 s exposure (open triangles), 120 s exposure (filled circles), and 300 s exposure (open circles) in 0.10 mM OPA solution. The average coverage for the three exposure times is 0.047, 0.131, and 0.182, respectively. The inset is an expanded view of the large island size distribution.

times. This is consistent with the formation of islands of a specific size during removal. The peak height is smaller at later times because not all the molecules deposited during removal become part of new islands—some attach to previously existing islands (formed while in solution). Greater numbers of large islands are observed after longer immersion. This is demonstrated by the increasing intensity in the tail of the distribution for large island sizes (see inset).

The island size distribution obtained from in situ images of growth (see Figure 7) is distinctly different from that of the quenched films. The coverage of the film in Figure 7 is similar to that of the quenched film immersed for 120 s from Figure 6. However, the island size distribution of the quenched film is peaked at about 200 nm^2 with a slowly decaying tail, while the distribution for the in situ image has a fairly symmetrical peak centered at about 500 nm^2. These differences are indicative of the removal process and consistent with the deposition of additional molecules during removal. Some of these molecules nucleate new islands with a typical area of 200 nm^2; others attach to preexisting islands, increasing their size and skewing the distribution.

As mentioned above, the average surface coverage, for "dipped" films increased monotonically with solution concentration, consistent with a greater surface density of OPA molecules. We also observed a systematic trend in the surface morphology of dipped films with solution concentration. Both the number density of islands and the mean island size increased with surface coverage (see Figure 8). These parameters are clearly influenced by the mechanism of island formation during removal. For example, they will be sensitive to the relative rates of island nucleation, surface transport, and island growth. We believe that this process lends itself well to simple modeling and we plan to perform Monte Carlo calculations in an attempt to understand the mechanisms better.

Analysis of Growth Kinetics. On the basis of the wetting, IR, and AFM data, including previously published in situ observations of submonolayer island growth,[7] we have formulated a hypothetical picture of monolayer formation consisting of several parts: bulk solution transport, adsorption onto the substrate surface, surface transport, and two-dimensional island growth (nucleation, growth, coalescence, etc.). Since we are observing films removed from solution, we must also consider the effect of removal. Quantitative analysis of the AFM images of incomplete films has allowed us to extract data related to

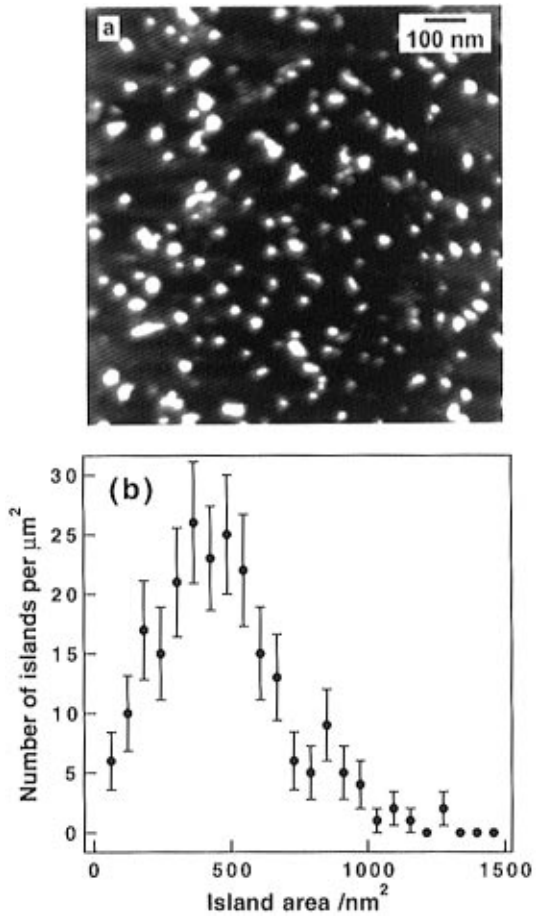

Figure 7. (a) AFM image, 1 μm × 1 μm, obtained in situ during monolayer growth on mica in a 0.05 mM OPA solution after about 20 min of exposure. The higher areas (lighter shades of gray) correspond to islands of OPA whose tops are about 2 nm higher than the surrounding substrate. (b) Island size distribution for the image shown in (a). There is a distinct peak at about 500 nm^2. The fractional coverage of the surface by islands is 0.14.

monolayer growth kinetics over a wide range of solution concentrations. One advantage of this method is that it is applicable even in the very early stages of growth—a particularly useful regime for testing kinetic models.

A generic fitting function for the coverage data has the form

$$\chi = f(t,c) + \lambda(c)(1 - f(t,c))$$

where c refers to solution concentration and λ is the amount deposited during removal (quasi-LB deposition) on a clean substrate and will be used as a free parameter during fitting. The function f describes the kinetics of the island growth in solution. The second term represents the amount deposited during removal ($(1 - f)$ is the amount of free surface at the time of removal). Note that inverting this expression yields

$$f = (\chi - \lambda)/(1 - \lambda)$$

This will be used later to collapse the data obtained at various concentrations onto the same plot.

We were originally motivated by the simplistic approximation that the island growth might be limited by the amount of material adsorbed from solution. As a result we have used two forms for f that are appropriate for adsorption kinetics. Parameters that must be considered in adsorption include the diffusion coefficient, D, the concentration, c, and the adsorption rate constant (sticking coefficient), K. A useful length scale to define is the height of a column of solution containing sufficient

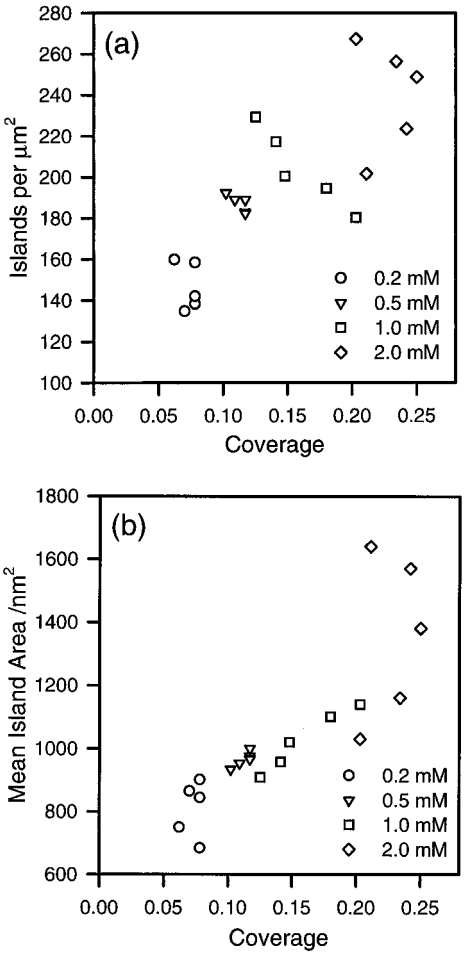

Figure 8. Dependence of (a) the number of islands per μm^2 and (b) the mean island size, for "dipped" films, upon solution concentration and total coverage.

molecules to cover the surface at equilibrium, l_D. Assuming a molecular area on the surface of 25 Å^2, we obtain $l_D \approx 6.7 \times 10^{-7}/c$. The time scale relevant to diffusive transport is, therefore, equal to $T_D = l^2/D$ and can be calculated reasonably well. For very large values of K the adsorption kinetics are controlled by diffusion only. The appropriate expression for diffusion-controlled kinetics (in a stagnant liquid) has been given as[17−19]

$$f(t,c) = 1 - \exp(t/T_D)\mathrm{erfc}((t/T_D)^{1/2})$$

Note that, in principle, there are no unknown parameters in this function. However, we will use T_D as a fitting parameter. For short times this expression can be written

$$f(t,c) \approx \left(\frac{4D}{\pi l_D^{\,2}}\right)^{1/2} t^{1/2}$$

In the opposite approximation (small K) the kinetics are dominated by the adsorption rate. A standard kinetic expression for this regime, consistent with the Langmuir isotherm at equilibrium, is[16,19]

$$f(t,c) = 1 - \exp(-cKt)$$

or for short times

$$f(t,c) \approx cKt$$

This expression contains the unknown parameter K.

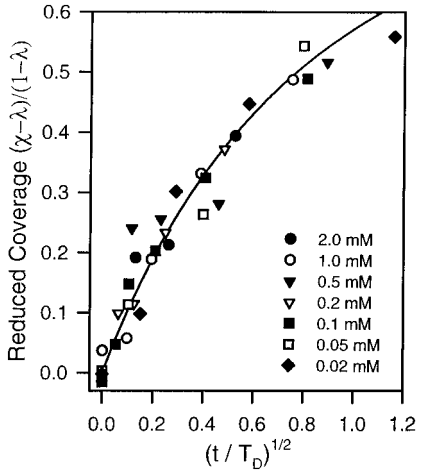

Figure 9. Fit of the data to the diffusion-limited model. The plot shows the reduced coverage, $(\chi - \lambda)/(1 - \lambda)$ versus $(t/T_D)^{1/2}$ for samples immersed in OPA solutions (in THF) with concentrations ranging from 0.02 to 2 mM. The best-fit values of λ and T_D for each concentration were used to collapse the data. The solid line represents the diffusion-limited kinetics model discussed in the text.

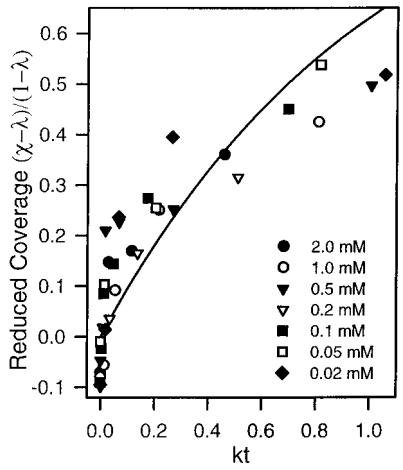

Figure 10. Fit of the reduced coverage data to the adsorption-limited model discussed in the text. The best-fit values of λ and K for each concentration were used to collapse the data. The solid line represents the adsorption-limited model. There are clear systematic deviations of the data from the model.

We have attempted to fit our data to fitting functions based on each of these models. Each data set, corresponding to a particular solution concentration, was fit to each function separately. For the diffusion-limited model, T_D and λ were used as free parameters. For the adsorption-limited model, K and λ were allowed to float. To display the general quality of fit for the two functions, we have collapsed all of the data onto one plot in each case. In both cases we plot the quantity $(\chi - \lambda)/(1 - \lambda)$ versus the appropriately scaled time variable t/T_D for the diffusion-limited case and Kt for the adsorption-limited case. The best-fit values of λ, T_D, and K were used for each concentration. The diffusion-limited model fit the data reasonably well (Figure 9), particularly below coverages of about 0.6. Discrepancies at high coverage are expected, since additional transport processes, such as convection, would become increasingly important. However, there was clear systematic disagreement between the data and the adsorption-limited model (Figure 10). This was somewhat surprising to us, since a previous paper on SAM kinetics had reported a general consistency with this model.[20] However, the data on which these conclusions were based were not particularly strong at short times, and, of course, the models are distinguished most easily in this

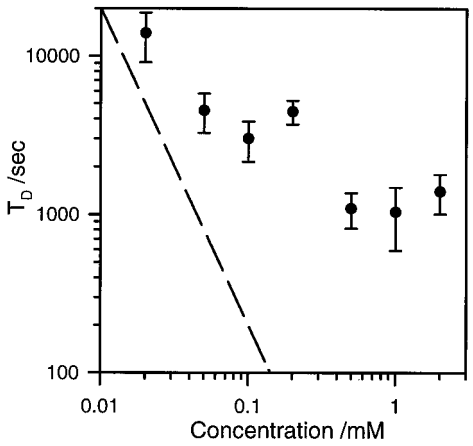

Figure 11. A log−log plot of the diffusion time scale, T_D, versus concentration, obtained from fitting the diffusion-limited model to the coverage data. The dashed line represents the time scale predicted by molecular diffusion in bulk solution, $T_D \approx 2 \times 10^{-6}c^{-2}$. At low concentrations the actual growth rate constant appears to approach the bulk solution value, while at higher concentrations the growth rate is clearly limited by a process slower than solution diffusion.

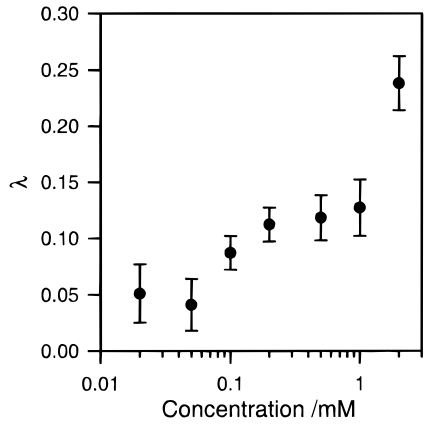

Figure 12. Semilog plot of the quasi-LB deposition parameter, λ, versus concentration. The general increase with increasing concentration is qualitatively consistent with the expected dependence of the surface density of surfactant molecules in a Gibbs monolayer.

regime. In any case, our data are inconsistent with an adsorption-limited (Langmuir) model for growth kinetics.

Although the data are consistent with kinetics following the diffusion-limited form, the values of T_D extracted from the fits are not consistent with bulk solution diffusion of individual molecules. Diffusion constants for molecules the size of OPA in THF generally lie in the range $10^{-7}-10^{-6}$ cm^2/s. An approximate calculation using a Stokes-type expression yields numbers in the range 2×10^{-7} to 5×10^{-7} cm^2/s. Using a conservatively small value of 2×10^{-7} cm^2/s, we calculate the expression $T_D = l_D^2/D \approx 2 \times 10^{-6}/c^2$, where c is given in mol/L. For the range of concentrations used, T_D should range between 0.5 and 5000 s. However, the measured range is 870−11 000 s (see Figure 11). In addition, T_D does not have the expected c^{-2} dependence. Our inevitable conclusion is that bulk solution diffusional transport is not the limiting factor in the monolayer growth. Since we have already ruled out adsorption-limited kinetics, this leads us to believe that the growth kinetics are controlled not by solution transport or adsorption but by the process of two-dimensional "self-assembly." We speculate that the agreement with the functional form for diffusion-limited kinetics may point to the importance of *surface diffusion* as a kinetic limitation during growth. The values of λ (associated with quasi-LB transfer) that were extracted from the fits are plotted versus c in Figure 12. The general increase with concentration is consistent with an increasing molecular density in the Gibbs monolayer.

We should note that the importance of surface diffusion was previously demonstrated in the growth of octadecyltrichlorosilane (OTS) monolayers.[9] In this system, islands were also observed in partial monolayers. These islands were fractal in shape, with a scaling exponent of about 1.7, consistent with *2-dimensional* diffusion-limited aggregation. Therefore, in the case of OTS growth, the importance of surface diffusion was inferred from the morphology of submonolayer islands. In the case of OPA, the growth kinetics suggests that surface diffusion is, again, the limiting process.

Conclusions

AFM images of quenched incomplete OPA SAMs suggested a growth process consisting of nucleation, growth, coalescence, etc., of densely packed molecules. Previous in situ AFM observations support this picture. The wettability of the incomplete films, by deposition solution (degree of autophobicity) and by water, as a function of coverage was consistent with the surface coverage implied by AFM images. IR spectroscopy data also supported the idea of densely packed islands of OPA surrounded by bare substrate. Quantitative coverage data were extracted from AFM images for solution concentrations in the range 2×10^{-5} to 2×10^{-3} M. The fact that the coverage did not extrapolate to zero at zero immersion time suggested that molecules were deposited during removal via a quasi-LB deposition process. This conclusion was buttressed by the measured surface tension of the deposition solution as a function of concentration (suggesting the presence of an adsorbed Gibbs monolayer) and the distinctive differences between the island size distributions of quenched versus in situ incomplete monolayers. Surprisingly, the details of the growth kinetics were found to be inconsistent with adsorption-limited (Langmuir) kinetics. A functional form appropriate for diffusion-limited adsorption kinetics was in good agreement with the observed coverage. However, the values of the diffusive growth time scale extracted from the fits were greater than expected for simple molecular diffusion and did not have the correct dependence on concentration. The quantitative failure of these two models implies that the kinetics were limited not by bulk transport or adsorption but by a two-dimensional transport (possibly surface diffusion) or assembly process.

Acknowledgment. We thank Abraham Ulman for preparation of the OPA. This work was supported by the National Science Foundation (Grant No. CHE-9614200), the donors of the Petroleum Research Fund, the Center for Photoinduced Processes (funded by the National Science Foundation and the Louisiana Board of Regents), and the Louisiana Education Quality Support Fund Contract LEQSF(1996-99)-RD-B-12.

References and Notes

(1) Camillone, N.; Eisenberger, P.; Leung, T. Y. B.; Schwartz, P.; et al. *J. Chem. Phys.* **1994**, *101*, 11031−11036.
(2) Poirier, G. E.; Tarlov, M. J.; Rushmeier, H. E. *Langmuir* **1994**, *10*, 3383−3386.
(3) Poirier, G. E.; Tarlov, M. J. *Langmuir* **1994**, *10*, 2853−2856.
(4) Fenter, P.; Eisenberger, P.; Liang, K. S. *Phys. Rev. Lett.* **1993**, *70*, 2447−2450.
(5) Allara, D. L.; Parikh, A. N.; Judge, E. *Chem. Phys.* **1994**, *100*, 1761−1764.
(6) Parikh, A. N.; Allara, D. L.; Azouz, I. B.; Rondelez, F. *J. Phys. Chem.* **1994**, *98*, 7577−7590.
(7) Woodward, J. T.; Schwartz, D. K. *J. Am. Chem. Soc.* **1996**, *118*, 7861.
(8) Woodward, J. T.; Ulman, A.; Schwartz, D. K. *Langmuir* **1996**, *12*, 3626.

(9) Schwartz, D. K.; Steinberg, S.; Israelachvili, J.; Zasadzinski, J. A. N. *Phys. Rev. Lett.* **1992**, *69*, 3354−3357.
(10) Bain, C. D.; Troughton, E. B.; Tao, Y.-T.; Evall, J.; et al. *J. Am. Chem. Soc.* **1989**, *111*, 321−335.
(11) Brochard-Wyart, F.; deGennes, P. G. *Adv. Colloid Interface Sci.* **1992**, *39*, 1.
(12) Elender, G.; Sackmann, E. *J. Phys. II* **1994**, *4*, 455.
(13) Redon, C.; Brochard-Wyart, F.; Rondelez, F. *Phys. Rev. Lett.* **1991**, *66*, 715.
(14) Cassie, A. B. D. *Discuss. Faraday Soc.* **1952**, *75*, 5041.
(15) Cameron, D. G.; Dluhy, R. A. In *Spectroscopy in the Biomedical Sciences*; Gendreau, R. M., Ed.; CRC Press: Boca Raton, FL, 1986; p 53.
(16) Adamson, A. W. *Physical Chemistry of Surfaces*, 5th ed.; John Wiley & Sons: New York, 1990.
(17) Frisch, H. L.; Mysels, K. J. *J. Phys. Chem.* **1983**, *87*, 3988−3990.
(18) Mysels, K. J.; Frisch, H. L. *J. Colloid Interface Sci.* **1984**, *99*, 136−140.
(19) Chang, C.-H.; Franses, E. I. *Colloids Surf. A* **1995**, *100*, 1.
(20) Cheng, S. S.; Scherson, D. A.; Sukenik, C. N. *J. Am. Chem. Soc.* **1992**, *114*, 5436−5437.